Engineering Fracture Mechanics 217 (2019) 106542

Contents lists available at ScienceDirect

Engineering Fracture Mechanics

journal homepage: www.elsevier.com/locate/engfracmech

Hydrogen informed Gurson model for hydrogen embrittlement simulation

Haiyang Yu[a,b], Jim Stian Olsen[a], Antonio Alvaro[c], Lijie Qiao[d], Jianying He[a], Zhiliang Zhang[a,*]

[a] Department of Structural Engineering, Norwegian University of Science and Technology, 7491 Trondheim, Norway
[b] Department of Materials, University of Oxford, Parks Road, OX1 3PH, UK
[c] SINTEF Materials and Chemistry, 7456 Trondheim, Norway
[d] Beijing Advanced Innovation Center for Materials Genome Engineering, Corrosion and Protection Center, University of Science and Technology Beijing, Beijing 100083, China

ARTICLE INFO

Keywords:
Hydrogen enhanced localized plasticity
Hydrogen-microvoid interaction
Gurson model
Void growth

ABSTRACT

Hydrogen-microvoid interactions were studied via unit cell analyses with different hydrogen concentrations. The absolute failure strain decreases with hydrogen concentration, but the failure loci were found to follow the same trend dependent only on stress triaxiality, in other words, the effects of geometric constraint and hydrogen on failure are decoupled. Guided by the decoupling principle, a hydrogen informed Gurson model is proposed. This model is the first practical hydrogen embrittlement simulation tool based on the hydrogen enhanced localized plasticity (HELP) mechanism. It introduces only one additional hydrogen related parameter into the Gurson model and is able to capture hydrogen enhanced internal necking failure of microvoids with accuracy; its parameter calibration procedure is straightforward and cost efficient for engineering purpose.

1. Introduction

Continuum level hydrogen embrittlement (HE) simulation is one of the key aspects of failure assessment and control of engineering components exposed to hydrogen environment. A sound framework for this purpose consists of three basic ingredients, namely a plausible underlying HE mechanism, a way to determine model inputs from experiments or lower scale simulations and eventually a continuum model applicable to various geometries and loading conditions. The underlying mechanism provides the physical foundation, the input calibration method serves as a bridge linking lower scale physics (often posed in a discrete manner) and continuum mechanics, and the model as the main carrier needs to be selected depending on the other two elements.

To date, there are two prevailing HE mechanisms, hydrogen enhanced decohesion (HEDE) and hydrogen enhanced localized plasticity (HELP). The HEDE mechanism assumes that dissolved hydrogen reduces the cohesive strength of the material lattice [1]; the HELP mechanism assumes that hydrogen facilitates dislocation activity thereby enhancing plasticity locally [2]. It is straightforward to see that HEDE is compatible with Griffith type fracture, so it is favorable for the simulation of HE which is usually accompanied by brittle-like fractography [3]. In fact, HEDE based continuum level HE simulation has been in progress for over a decade, thanks to cohesive zone modeling (CZM) which well represents the brittle fracture process [4]. By lowering the cohesive strength (fracture energy) of the cohesive interface with hydrogen content, hydrogen induced premature fracture in a brittle manner

* Corresponding author.
E-mail address: zhiliang.zhang@ntnu.no (Z. Zhang).

https://doi.org/10.1016/j.engfracmech.2019.106542
Received 10 February 2019; Received in revised form 20 June 2019; Accepted 1 July 2019
Available online 18 July 2019

Nomenclature

$\dot{f}$	void growth rate
η	stress triaxiality
$\overline{V}_h$	partial molar volume of hydrogen
σ_0	initial yield stress without hydrogen
σ_e	equivalent stress
σ_h	hydrostatic stress
ε_0	strain at yielding
ε_e	effective strain
ε_f	failure strain
ε_p	plastic strain
c	hydrogen concentration
c_L	lattice hydrogen concentration
c_T	trapped hydrogen concentration
D_L	hydrogen diffusion coefficient
E	Young's modulus
E_b	trap binding energy
f_0	initial void volume fraction
f_c	critical void volume fraction
R	universal gas constant
T	absolute temperature

can be simulated. The determination of CZM parameters in the absence of hydrogen is out of the scope and not elaborated here. Hydrogen related inputs, i.e. hydrogen effects on CZM parameters, can be obtained based on atomistic calculations or experiments. Jiang and Carter [5] performed first principles calculations and found that the ideal fracture energy decreases almost linearly with increasing hydrogen coverage. This relation was then adopted by Serebrinsky et al. [6] and Olden et al. [7] in their hydrogen informed CZM (HCZM) simulations. Recently, Yu et al. [8] proposed a method to calibrate hydrogen dependent cohesive laws from tension tests. The HCZM approach is now rather mature and applied widely to engineering failure assessment [9,10]. Following a similar pattern, the phase field approach was recently applied in HE simulation [11]. In spite of its popularity, HCZM has intrinsic deficiencies. While it "physically" represents the brittle failure caused by hydrogen, it cannot represent the ductile damage in the absence of hydrogen. Due to this inconsistency, it has to be admitted in the first place that HCZM is a phenomenological approach.

In contrast to the great popularity of the HELP mechanism, HELP based continuum model for hydrogen failure prediction is yet to be developed. There could be several reasons. First, the HELP mechanism claims more plasticity in the presence of hydrogen, so one may expect ductile fracture all the time, which doesn't agree with the brittle-like HE fractography. Therefore, one could intuitively prefer HEDE to HELP as the underlying mechanism for continuum HE modeling. Secondly, unlike the HEDE case where the DFT results of hydrogen dependent cohesive law can be readily applied to the continuum level, the HELP mechanism, while verified by theoretical calculation using a pair of dislocations [2], cannot be quantitatively applied to the continuum level, since plasticity is the collective behavior of a large dislocation aggregate on which the hydrogen effect is still unclear. Finally, even if a phenomenological form for the HELP mechanism is temporarily assumed and implemented in unit cell analyses [12], the results are only qualitative ones due to the lack of a proper failure criterion. In short, a HELP based continuum model is still lacking because the underlying theory seems inconsistent with reality and a bridge linking different scales is lacking.

The conditions for the development of HELP based continuum model has been largely improved recently. Yu et al. [13] proposed a failure criterion associated with hydrogen induced shear band forming in unit cell analysis, which allows failure to be detected at a very small void volume fraction at low stress triaxiality regime. That is, hydrogen induced premature failure with brittle-like fractography was predicted under the HELP mechanism solely. That work also demonstrated that more plasticity does not necessarily lead to higher ductility, it therefore removed the first obstacle for adopting HELP in a continuum model. Further, a hydrogen failure locus covering a wide range of stress triaxiality was established in that work, providing inputs for the continuum model. Meanwhile, it should be noted that the link between continuum scale and lower scales is still weak, since the HELP mechanism is implemented only conceptually using a phenomenological form in the cell analyses performed so far. Most recently, a hydrogen informed three dimensional discrete dislocation dynamics (HDDD) modeling framework was established [14], incorporating the elastic stress contribution from hydrogen as Eshelby inclusion [15] and hydrogen effects on dislocation mobility calibrated based on first principles calculations [16]. Global flow behavior was simulated with this method using a microcantilever geometry and hydrogen induced global softening, consistent with the HELP mechanism, was quantitatively captured at realistic bulk hydrogen concentrations. This framework addresses hydrogen influenced large dislocation aggregate property (plasticity) at microscopic scale and can therefore serve as an ideal bridge between the atomistic and continuum scales.

With the theoretical foundation and inter-scale bridge established, the construction of HELP based continuum model is now on the agenda. Although such model is still unavailable, lots of work on the mechanics of hydrogen induced failure due to HELP has been done, providing mechanistic insights. Sofronis et al. [17] introduced HELP to mechanical analyses by implementing a hydrogen softening law which prescribes the material yield stress as a decreasing function of hydrogen concentration. This method was then adopted by Ahn et al. [12], Liang et al. [18] and implemented in unit cell analyses. By zooming into a material point represented by a void containing representative material volume, the unit cell approach is an ideal tool to investigate material failure characterized by microvoid growth and coalescence process [19]. With hydrogen softening the matrix flow stress, material failure by void coalescence along the inter-ligament was found to occur earlier, i.e. hydrogen promoted internal necking failure. In [13], a hydrogen induced shearing failure mode was identified and quantified. This failure mode is observed in low stress traxiality regime and occurs with a much smaller void size compared to that in the internal necking mode, therefore, it captures the "embrittlement" feature of hydrogen caused failure. Most recently, Huang et al. [20] studied the effect of hydrogen under different Lode parameters with unit cell approach. These studies reveal the micromechanics of hydrogen caused premature failure under the HELP theory, with a merit that the basic failure process is consistently based on microvoid activity with or without hydrogen. Therefore, they open the door to a consistently micromechanics based continuum model which could be an alternative to the phenomenological HCZM framework for

continuum HE modeling.

Given the background above, the Gurson model [21] seems to be an ideal starting point for a HELP based continuum model for HE simulation. This model describes the "average" flow behavior of a single void containing representative material volume (unit cell) during the development of the void (growth and coalescence), by "smearing" the void throughout the unit cell and then viewing the smeared cell as a material point. Regarding void coalescence as the failure event, the Gurson model is able to predict failure if a critical void volume fraction is accordingly prescribed [22]. An alternative way to predict failure is to incorporate a physically based void coalescence criterion [23–25] to the Gurson model. During the past decades, a lot of improvement and adaption have been made on this model, breeding many different versions. In general, we refer to all the versions in this family as the Gurson model. Specifically, we based our discussion on the version developed by Tvergaard and Needleman [22] in this work. The Gurson model elegantly applies the mechanics happening locally in a unit cell to global specimen level and has achieved great success in engineering practice. It is also an ideal starting point for developing new microvoid mechanism based models, for which the modification of the Gurson model for shear [26] is a typical example. About one decade ago, it was realized that the ductile failure locus is dependent not only on stress triaxiality but also on the Lode parameter [27], and this was then studied extensively using unit cell approach [28,29]. Inspired by the micromechanics revealed in cell analyses, Nahshon and Hutchinson [26] introduced a Lode parameter dependent term to the void growth rate term, making material failure shear sensitive. Essentially, this new model regards void volume fraction as a continuum damage parameter which is made additionally dependent on Lode parameter. Therefore, this model is not as well physically based as the original Gurson model, nevertheless, it is still micromechanism inspired and is widely adopted in practice [30]. Similar treatment on the Gurson model is found in [31,32].

The present work discusses the possibility of using the Gurson model to convey hydrogen-microvoid interaction mechanisms to the continuum scale. Should this work, a micromechanics inspired HELP based continuum modeling tool for HE can be delivered. This potential model is referred to as the hydrogen informed Gurson (HGurson) model hereinafter. Starting from hydrogen-microvoid interactions, a possible form of HGurson model is proposed, together with a suitable parameter calibration procedure. At the moment, we don't aim to deliver a complete HGurson model ready for use, given the complexity in hydrogen assisted microvoid failure process. Instead, we elaborate the challenges in the development of such a model, propose solutions for some of them and leave the rest for future study. As a brief overview, the challenges/complexities include (but are not limited to): hydrogen trapping, change of failure mode in different stress triaxiality regime, inhomogenous material softening due to hydrogen redistribution and the form of hydrogen softening law. Being aware of all these complexities, we hereby limit our focus to a simple case with a linear softening law in high triaxiality regime, and a prototype HGurson model is presented.

2. Hydrogen-microvoid interactions

Hydrogen microvoid interactions are investigated via hydrogen diffusion coupled unit cell analyses [13]. J2 flow theory with isotropic hardening is applied to describe the plastic flow in the matrix material

$$\sigma_f = \sigma_0(c)\left(1 + \frac{\varepsilon_p}{\varepsilon_0}\right)^n \tag{1}$$

where σ_f is the flow stress, $\sigma_0(c)$ the initial yield stress which is a function of the total hydrogen concentration c, ε_p the plastic strain and $\varepsilon_0 = \sigma_0/E$ the corresponding yield strain with E being the Young's modulus. To account for the HELP mechanism, the flow stress in the matrix material is assumed to decrease with hydrogen content. More specifically, the initial yield stress σ_0 is prescribed as a decreasing function of hydrogen concentration, for which the linear form [12] is most widely adopted

$$\sigma_0(c) = \begin{cases} \left[\left(\xi - 1\right)\frac{c}{c_L^0} + 1\right]\sigma_0 & \sigma_0(c) > \zeta\sigma_0 \\ \zeta\sigma_0 & \sigma_0(c) \leqslant \zeta\sigma_0 \end{cases} \tag{2}$$

where σ_0 is the initial yield stress with zero hydrogen concentration, $\xi\sigma_0$ the initial yield stress at the initial lattice hydrogen concentration c_L^0 and $\zeta\sigma_0$ the lowest possible value of the yield stress considering that hydrogen cannot cause the yield stress to vanish in reality.

The total hydrogen population consists of the lattice hydrogen residing at normal interstitial lattice sites and the trapped hydrogen residing at dislocation traps

$$c = c_L + c_T \tag{3}$$

where c_L is the lattice hydrogen concentration and c_T the trapped hydrogen concentration. These two quantities can be further expressed as

$$c_L = \theta_L N_L \qquad c_T = \theta_T N_T \tag{4}$$

where θ_L is the fraction of occupied interstitial lattice sites and N_L the lattice site density; similarly, θ_T is the fraction of occupied trapping sites and N_T the trapping site density.

Assuming steady state hydrogen distribution, the material flow stress is dependent on the hydrostatic stress field and the plastic strain field, which can be implemented to realize hydrogen coupled unit cell analysis [12]. Alternatively, transient hydrogen diffusion analysis can be directly coupled with unit cell analysis [13], which can be realized with the help of user subroutines in a commercial

finite element software such as ABAQUS [33]. Under the limit of sufficient diffusion time, these approaches are equivalent, and the latter is adopted in this work. Transient hydrogen diffusion is governed by

$$\frac{\partial c_L}{\partial t} + \frac{\partial c_T}{\partial t} - \nabla\cdot\left(D_L \nabla c_L\right) + \nabla\cdot\left(\frac{D_L c_L \overline{V}_h}{RT}\nabla\sigma_h\right) = 0 \tag{5}$$

where D_L stands for the lattice diffusivity coefficient, $\overline{V}_h$ the partial molar volume of hydrogen and σ_h the hydrostatic stress. An equilibrium exists between hydrogen in lattice sites and in trapping sites [34]

$$\frac{\theta_T}{1-\theta_T} = \frac{\theta_L}{1-\theta_L} K_T \tag{6}$$

where K_T is the trap equilibrium constant $K_T = exp(-E_b/RT)$ with E_b being the trap binding energy, R the universal gas constant and T the absolute temperature.

The unit cell method focuses on a single void behavior in a representative material volume with periodic boundary condition. It offers accurate control over loading path and is an ideal approach to construct material failure loci [35]. The failure locus is defined as a relation between the effective strain at failure ε_f and the geometric constraint. The level of geometric constraint can be characterized by stress triaxiality and Lode parameter [13]. In this work, the cylindrical unit cell [19] under proportional loading is employed, leading to an axisymmetric loading scenario where the Lode parameter remains constant $L \equiv -1.0$. In other words, 2D failure loci are concerned throughout this work. The effective strain of the unit cell is defined as [19]

$$\varepsilon_e = \frac{2}{3}|\varepsilon_3 - \varepsilon_1|, \tag{7}$$

where $\varepsilon_3 = ln(L/L_0)$ and $\varepsilon_1 = ln(R/R_0)$, with L and R being the current cell height and radius, respectively. And the level of constraint is characterized by stress triaxiality

$$\eta = \frac{\sigma_h}{\sigma_e}, \tag{8}$$

with σ_e being the equivalent stress.

With a similar approach, we studied the effect of hydrogen on material failure loci in a previous work [13] and a complicated picture was revealed. The effect was found to depend on hydrogen trap strength as well as stress triaxiality. With weak trapping, failure occurred in internal necking mode over the entire range of triaxiality, and hydrogen promoted this failure mode. With strong trapping, hydrogen induced the formation of a shear band in the low triaxiality regime, giving rise to a new internal shearing failure mode. This adds complexity to the development of the HGurson model. Ultimately, a successful HGurson model is expected to reproduce the hydrogen failure loci, capturing all the complexities involving trapping strength dependency and different failure modes. This work as a starting point, is devoted only to capturing hydrogen promoted internal necking failure mode, which is the first issue that should be addressed in model development. In other words, we limit our focus here to the medium and high stress triaxiality regime $\eta > 1.0$.

Hydrogen diffusion coupled unit cell analysis describes the mechanical process in a representative material volume, which is viewed as a material point at the specimen level. Therefore, HGurson model is essentially a homogenized description of hydrogen-microvoid interactions at material points. In this sense, the cell analyses can be regarded as “virtual experiments” that can be used as reference to calibrate and validate the HGurson model. Such “virtual experiments” need to be performed with various hydrogen concentrations. In all the cell analyses here, the Young’s modulus is $E = 2 \times 10^5$ MPa, the initial yield stress of the material is $\sigma_0 = 400$ MPa, and the strain hardening exponent is $n = 0.1$. The initial void volume fraction of the unit cell is $f_0 = 0.0013$ in all

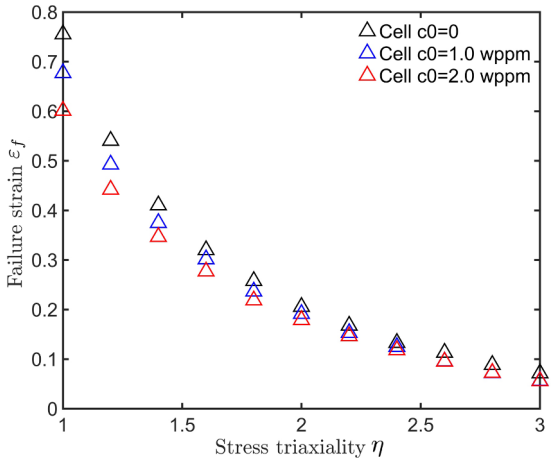

Fig. 1. The failure loci obtained by hydrogen diffusion coupled unit cell analyses, with and without hydrogen.

simulations. The linear hydrogen softening law in Eq. (2) is adopted with $\xi = 0.9$ and $\zeta = 0.5$. Lattice hydrogen properties relevant to steel are adopted: the lattice site density is taken as $N_L = 8.74 \times 10^{19}$ sites/mm^3, the partial molar volume of hydrogen as $\overline{V}_h = 2 \times 10^3$ mm^3/mol and lattice diffusion coefficient as $D_L = 2.5 \times 10^{-11}$ m^2/s. The same trapping parameters as in [13] representing a strong trapping scenario are adopted. The reference hydrogen concentration (Eq. (2)) at which a 10% reduction in yield stress is observed is assumed to be $c_L^0 = 1.0$ wppm. The loading rate during simulation is sufficiently low so that steady state hydrogen distribution is guaranteed. It should be noted that the assumed level of hydrogen softening is very large. This is for a larger contrast between hydrogen and original failure loci and for a better demonstration of the decoupling principle. With less softening, the principle and the HGurson model still apply well, except that the absolute difference in the failure loci is less pronounced. To give a sense of how the magnitude of the effect of hydrogen depends on the softening parameters, we include unit cell results with milder hydrogen softening, a 5% reduction and a 1% reduction with $c_L^0 = 1.0$ wppm, in Appendix A.

Four cases with different initial uniform hydrogen concentrations $c_0 = 0.5$, 1.0, 1.5, 2.0 wppm and a hydrogen free case $c_0 = 0$ are investigated. Unit cell analyses are performed under fixed stress triaxiality ranging from $\eta = 1.0$ to $\eta = 3.0$ with an interval of 0.2. Over this range, only hydrogen promoted internal necking failure is observed. The failure loci are constructed for each hydrogen concentration.

The results of hydrogen coupled unit cell analyses, quantified as failure loci, are presented in Fig. 1. Internal necking failure is observed over the entire range of triaxiality in all cases, and the failure strain decreases with the increase of hydrogen concentration.

Before establishing a model to capture these failure loci, the mechanism of hydrogen promoted internal necking failure needs to be analyzed. An intuitive impression is that hydrogen induced softening of the matrix material accounts for the early failure, since the initial yielding stress lowers as c_0 increases. Looking into the hydrogen distribution contour during the loading process, another possible reason is spotted. Due to the pressure and plastic strain dependent nature of hydrogen redistribution, higher hydrogen concentration is built up at the inter-ligament region, which in turn leads to non-uniform hydrogen softening across the unit cell, as shown in Fig. 2. This could also be a rationale for the premature failure. To distinguish between these causes, we refer to the former rationale as hydrogen caused uniform softening and the latter as hydrogen caused non-uniform softening.

To probe the actual cause, an artificial case where the initial yield stress of the matrix material is decreased uniformly by 50% (the lower bound of hydrogen softening) was simulated. The void growth curves in this case and in the realistic cases with and without hydrogen are plotted in Fig. 3. Clearly, hydrogen caused uniform softening in the matrix material contributes little to the acceleration in void growth and premature failure, indicating hydrogen caused non-uniform softening plays a dominant role. This provides important reference for subsequent model development.

3. HGurson formulation

Coming back to the failure loci in Fig. 1, it is observed that they generally follow a same trend, which is clearly demonstrated by applying a normalization scheme as shown in Fig. 4(a). The scheme was performed by normalizing the failure strain values on each failure locus by the value corresponding to $\eta = 1.0$ on the same locus. After normalization, all the failure loci, including the hydrogen free failure locus, collapsed into one curve, verifying that they have the same triaxiality dependence, so the presence of hydrogen just scales the absolute value of a specific locus. In other words, it indicates the failure strain $\varepsilon_f(\eta, c)$ which is a function of stress triaxiality and hydrogen concentration can be expressed in a decoupled form

$$\varepsilon_f(\eta, c) = f(\eta) \cdot h(c) \tag{9}$$

with $f(\eta)$ determined in Fig. 4(a) and $h(c)$ in Fig. 4(b). It should be noted that $h(c)$ is a "hydrogen scaling" function that is calibrated from the "virtual experiments" instead of a fitting parameter. The decoupling phenomenon has been observed in the case without

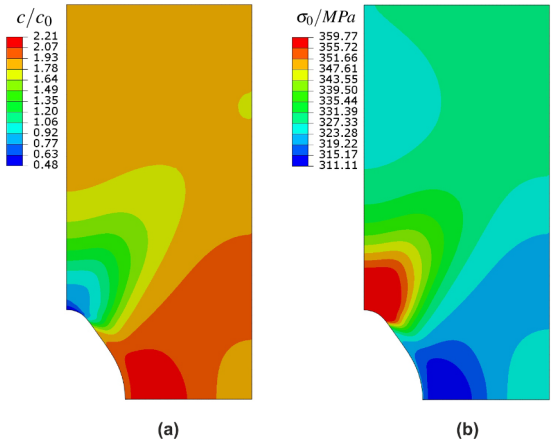

Fig. 2. (a) The distribution of hydrogen concentration and (b) the initial yield stress contours at an effective strain $\varepsilon_e = 0.5$ and stress triaxiality $\eta = 1.0$, obtained with hydrogen $c_0 = 1.0$ wppm.

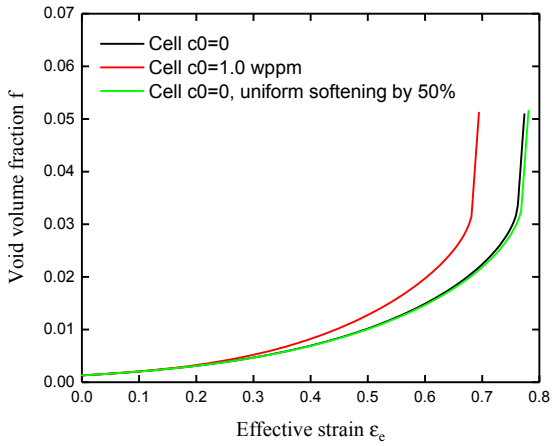

Fig. 3. Void growth curves obtained via unit cell analyses at stress triaxiality $\eta = 1.0$, including the hydrogen free case, a hydrogen case and an artificial case where no hydrogen is present but the entire matrix material is uniformly softened by 50%.

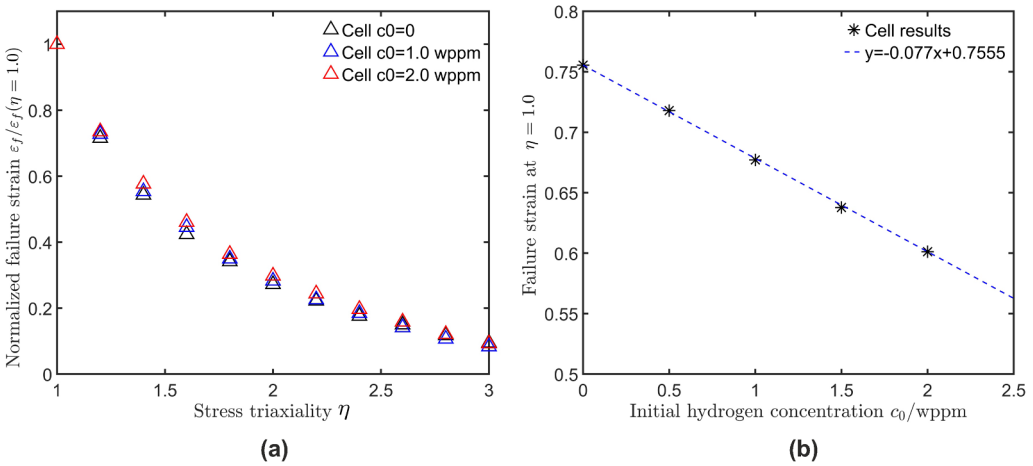

Fig. 4. (a) The normalized failure loci; the failure loci approximately collapse into one curve upon normalization. (b) The value used for normalization versus initial hydrogen concentration, which shows a linear relation.

trapping as well as in the current case. It may be attributed to the fact that the same failure mechanism, i.e. hydrogen induced local softening and the similar softening pattern, e.g. Fig. 2(b), apply at different hydrogen concentrations. This decoupling principle holds true as long as the hydrogen induced local softening occurs at the inter-ligament, which is the case in the high triaxiality regime concerned here. In the low triaxiality regime where internal shearing failure is observed [13], this principle needs to be verified separately. The fact that the hydrogen free case also follows this rule suggests that we can start from a hydrogen free mechanical model and then incorporate the scaling due to hydrogen to capture the hydrogen failure loci. To predict failure of microvoids without hydrogen, the Gurson model is a perfect candidate.

3.1. Gurson model

The Gurson model [36] is a popular approach to describing failure in porous materials. In 1975, Gurson [36] studied the macroscopic plastic flow of a long circular cylindrical void in a matrix of rigid-plastic von Mises material. By utilizing an approximate velocity field and appropriate boundary values at the outer and void surface, an upper bound yield function was derived

$$\phi\left(\boldsymbol{\sigma}, \bar{\sigma}, f\right) = \left(\frac{\sigma_e}{\bar{\sigma}}\right)^2 + 2q_1 f \cosh\left(\frac{q_2\sigma_m}{2\bar{\sigma}}\right) - 1 - q_3 f^2 = 0 \tag{10}$$

where $\boldsymbol{\sigma}$ is the stress tensor and f the void volume fraction; σ_e is the macroscopic equivalent stress and σ_m the mean stress. q_1, q_2 and $q_3 = q_1^2$ are the parameters introduced by Tvergaard and Needleman [22] in order to enhance the fitting capacity. This modified version is usually referred to as the GTN model [37], and the original Gurson model is retrieved by setting q_1, q_2 and q_3 to 1. In this model, the porous material is represented by a void free continuum, and the microvoids are "smeared" across the continuum.

When loaded, the void volume fraction f of the material increases due to microvoid growth, and the yield surface is modified

following Eq. (10). The rate of void volume change $\dot{f}$, i.e. void growth rate is derived from the mass conservation condition in the matrix

$$\dot{f} = (1-f)D_{kk}^{P} \tag{11}$$

where D_{kk}^{P} is the volumetric strain rate. It is assumed that failure initiates when the void volume fraction reaches a critical value $f = f_c$. Therefore, f could be regarded as a damage parameter with a sound micromechanical basis.

The GTN version is employed here to capture the microvoid failure locus in the absence of hydrogen. Consistent with the unit cell analyses, the material initially possesses a void volume fraction $f_0 = 0.0013$ and void nucleation is not taken into account. The same mechanical properties for the unit cell matrix are assigned to the Gurson matrix. Unit cell analyses show that the critical void volume fraction at failure initiation is around 0.03, therefore, $f_c = 0.03$ is adopted in the Gurson model. A single element model assigned with Gurson material is employed, in order to verify the predictions against the cell results. This element corresponds to the material point represented by the unit cell in Section 2. The same loading conditions, e.g. fixed stress triaxiality, are applied to the single element model as to the unit cell. The GTN fitting parameters are selected as $q_1 = 1.3$, $q_2 = 1.0$, $q_3 = 1.69$, which yields the best prediction of the hydrogen free failure locus. The Gurson model predictions of unit cell failure locus and void growth in the case of $\eta = 1.0$ are presented in Fig. 5. Good agreement between the model prediction and the cell results are achieved.

3.2. HGurson model

Following the decoupling principle revealed in the previous section, we now proceed to incorporate the effect of hydrogen into the Gurson model established above. Since the material point is represented by only one element in the HGurson model, hydrogen redistribution observed in the unit cell analyses cannot be directly captured. Therefore, the hydrogen concentration that is passed to the model has to be the initial uniform hydrogen concentration applied to the unit cell: again, the entire hydrogen-microvoid interactions, including hydrogen redistribution and plasticity localization are captured in a homogenized manner by the HGurson model. Recall that it is the hydrogen caused non-uniform softening that is dominant in the premature failure, but this cannot be reflected directly in the single element model. Looking at the derivation of the original Gurson model, we face the same dilemma: the Gurson model was derived assuming an isotropic matrix with uniform mechanical property, therefore, hydrogen can only soften the entire volume, in other words, there is no way to implement non-uniform hydrogen softening, if we wish to rigorously keep the original formulation of the Gurson model.

To demonstrate the deficiency of considering only the hydrogen caused uniform softening effect in HGurson model, we use a simple artificial case where the single element Gurson model is simulated at $\eta = 1.0$ and the initial yield stress of the matrix material is decreased by 50% uniformly. This artificial HGurson case corresponds to the artificial cell case in Fig. 3. The void growth curve has been included in Fig. 8(a). Clearly, directly implementing uniform softening to the Gurson model has little influence on void growth and therefore does not help capture the hydrogen failure loci.

To account for the hydrogen caused non-uniform softening effect in the HGurson model, the rigorous way is to reformulate the original Gurson model to consider a local softening regime in the void ligament. The solution will be extremely difficult, if not impossible, and it requires quantitative description of hydrogen induced non-uniform softening when it comes to the HGurson model, which induces further complexity. An alternative way is to view the Gurson model as a damage model and the void volume fraction f a damage parameter, so that the premature failure can be attributed to the hydrogen promoted accumulation of damage. The latter is adopted in this work, inspired by the practice in [26] which introduced the influence of external shearing to the Gurson model.

The strategy is therefore to let hydrogen accelerate damage accumulation in the Gurson model, and the acceleration should be dependent on hydrogen concentration. For this purpose, the void growth rate $\dot{f}$ is made additionally dependent on the initial hydrogen concentration c_0 applied to the material point. It should be noted that c_0 is referred to as the initial concentration in the sense

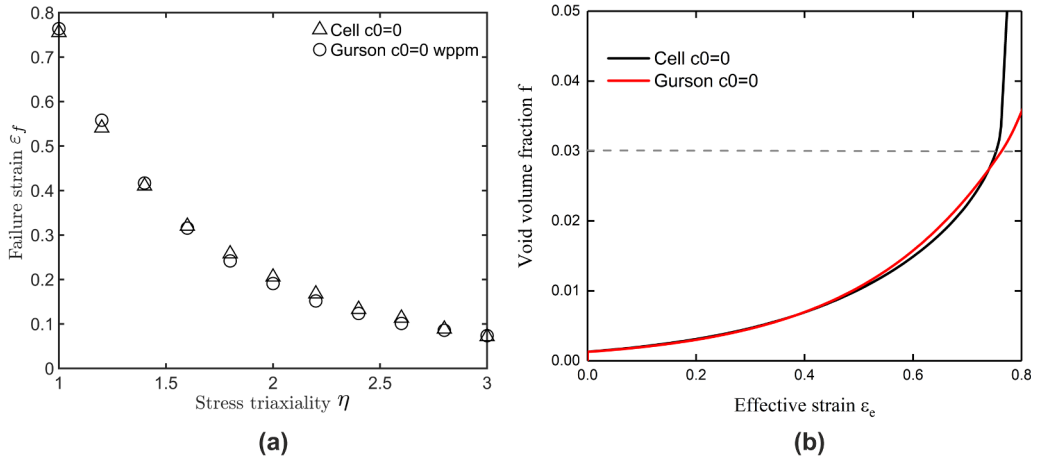

Fig. 5. Using the Gurson model to capture (a) hydrogen free failure locus and (b) void growth in the case with stress triaxiality $\eta = 1.0$.

that it prescribes the hydrogen condition at the beginning of hydrogen-microvoid interaction, at each material point and for a given time step in HGurson simulation. At the specimen level, c_0 should correspond to the transient hydrogen concentration at materials points instead of the global concentration initially applied to the whole specimen. In the lack of further information on hydrogen accelerated damage accumulation, the linear scaling function stands as a natural option [26]

$$\dot{f}(c_0) = \dot{f}_0 \cdot k_H(c_0) = (1-f) D_{kk}^P \cdot k_H(c_0) \tag{12}$$

As to be shown later, this function can yield satisfactory failure prediction. In this formulation, the void growth rate in the presence of hydrogen is simply the hydrogen free void growth rate $\dot{f}_0 = \dot{f}(c_0 = 0)$ multiplied by a scaler as a function of hydrogen concentration at the material point. In the case of the single element model, since the initial hydrogen concentration is constant, this scaler is a constant. Therefore, this scaler function can be calibrated via comparison between the single element model and unit cell results.

Applying Eq. (12) and keeping all the other parameters unchanged, the void growth rate will be accelerated. However, it is not easy to evaluate the acceleration analytically, since the volumetric strain rate D_{kk}^P in this expression will also be increased due to the modification. Assuming D_{kk}^P remains constant throughout the simulation, we have

$$\int_0^{\varepsilon_{f0}} \dot{f}_0 \, d\varepsilon = f_c \tag{13}$$

$$k_H(c_0) \cdot \int_0^{\varepsilon_f(c_0)} \dot{f}_0 \, d\varepsilon = f_c \tag{14}$$

where ε_{f0} denotes the hydrogen free failure strain. Eq. (14) indicates the hydrogen failure strain $\varepsilon_f(c_0)$ is equivalent to the strain value corresponding to the void volume fraction $f_c/k_H(c_0)$ in the hydrogen free case. In the simplest scenario where $\dot{f}_0$ is constant, i.e. the void growth curve is linear, we have

$$k_H(c_0) = \frac{\varepsilon_{f0}}{\varepsilon_f(c_0)} \tag{15}$$

In practice, however, the void growth curve is concave up as shown in Fig. 6. In this figure, the actual failure strains are $\varepsilon_f = 0.682$ and $\varepsilon_f = 0.764$ in the $c_0 = 1.0$ wppm and $c_0 = 0$ cases, respectively. Due to the linear void growth assumption, the scaler is determined as $k_H = 1.16$, yielding a prediction of $\varepsilon_f = 0.733$, ≈7.5% higher than the actual value. Therefore, the linear void growth assumption leads to overestimation. Meanwhile, it is noted that the discussion above is based on the assumption that D_{kk}^P remains constant after implementing Eq. (12). As a matter of fact, D_{kk}^P is found to increase in the simulation with hydrogen, scaled up approximately by a factor of $\alpha \cdot \varepsilon_e$, with $\alpha > 1.0$ roughly being a constant and ε_e the effective strain. This implies the failure strain predicted with Eqs. (14) and (15) in practice will be smaller than that estimated in Fig. 6. In other words, the overestimation eventually will be less than 7.5%, making the prediction rather satisfactory.

Going back to Fig. 4 and Eq. (9), we now have

$$k_H(c_0) = \frac{\varepsilon_f(\eta, 0)}{\varepsilon_f(\eta, c_0)} = \frac{h(0)}{h(c_0)}, \tag{16}$$

so the parameter k_H is a function of c_0 and independent of stress triaxiality. k_H as a function of c_0 can then be calibrated based on Fig. 4(b)

$$k_H(c_0) = 0.16 c_0 + 1.0. \tag{17}$$

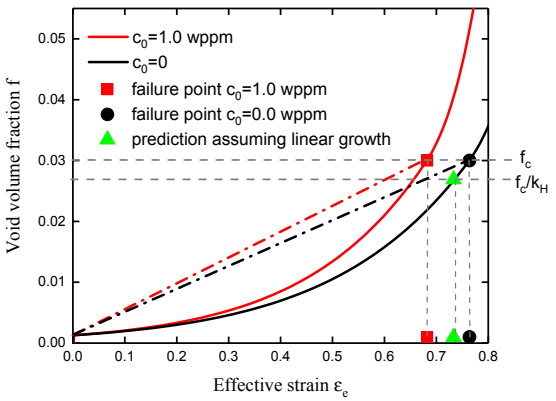

Fig. 6. The prediction of hydrogen failure point using Eq. (14) and assuming linear void growth. The solid lines represent the actual void growth curves extracted from HGurson simulations, and the dashed dotted lines represent the assumed linear void growth line. k_H is determined as $k_H = \frac{\varepsilon_{f0}}{\varepsilon_f\left(c_0 = 1.0 \text{ wppm}\right)}$.

It should be emphasized that this function is obtained via calibration of the unit cell failure loci following the decoupling principle, rather than out of pure fitting.

The HGurson model is established by implementing Eqs. (12) and (17). This model is then implemented via user defined material subroutine UMAT in ABAQUS [33], using the explicit consistent tangent modulus method [38–40]. The hydrogen failure loci predicted by the single element HGurson model for the cases $c_0 = 1.0$ wppm and $c_0 = 2.0$ wppm are shown in Fig. 7. Satisfactory agreement between the HGurson predictions and the unit cell results is achieved. Except for the failure strain, the void growth curve and stress-strain relation are also captured with good accuracy, which is verified by comparing the HGurson and unit cell results with $\eta = 1.0$ and $c_0 = 1.0$ wppm, as shown in Fig. 8.

So far, an HGurson model accounting for hydrogen enhanced internal necking failure has been delivered. This model reproduces the "virtual experimental" results obtained via hydrogen diffusion coupled unit cell analyses. For a given material, this model keeps all the hydrogen free material properties calibrated for the Gurson model and introduces only one additional hydrogen acceleration of void (damage) growth term $k_H(c_0)$, which is dependent only on hydrogen concentration c_0. In real life, the void behavior is more complicated, accompanied by rotation and shape change. These will inevitably affect model parameters, such as the critical void volume fraction f_c and the q parameters in the GTN version. To consider the hydrogen dependence of these parameters, more parameters and assumptions have to be included and additional calibrations are required, rendering the model redundant. Following the decoupling principle regarding the effect of hydrogen, we keep all the Gurson parameters unaffected by hydrogen, once they are determined in the hydrogen free case. This yields a clean HGurson model with good accuracy. Similar practice is found in the shear modified Gurson model [26]. As noted before, c_0 is the initial uniform hydrogen concentration in the single element model, but it will be the real time hydrogen concentration at material points in specimen level simulations. The application of Eq. (2) will cause softening to plastic flow, which will occur mainly at the failure process zone where a high concentration of hydrogen is built up. In most part of the specimen, hydrogen concentration will remain low and therefore the global loading curve is not expected to be severely softened.

The HGurson model is of practical value for engineering failure assessment to which material failure locus is critical. To calibrate a failure locus, the conventional way is to design test specimens with various geometries representing a range of stress triaxialities; the specimens are then loaded to failure so that the relation between failure strain and stress triaxiality can be obtained. For hydrogen failure assessment, the whole procedure has to be repeated under different hydrogen concentrations, in order to construct hydrogen failure loci as shown in Fig. 1, which increases the workload by several times. Inspired by the decoupling principle revealed in Fig. 4, the calibration procedure for the HGurson model and hence for failure loci can be significantly simplified:

(I) A series of mechanical tests with different geometries (stress triaxialities) in the absence of hydrogen need to be performed on a given material, yielding hydrogen free Gurson model parameters (hydrogen free failure locus), e.g. [41].
(II) Hydrogen charged mechanical tests need to be performed using any (one) geometry at several hydrogen concentrations to produce a hydrogen degradation curve similar to that in Fig. 4(b), and the hydrogen related term $k_H(c_0)$ (Eq. (17)) can then be determined.

In this procedure, different geometries need to be tested only in step (I), which is the necessary cost for material calibration in the absence of hydrogen. In step (II), utilizing the decoupling concept, only one specimen geometry is needed and only a couple of hydrogen concentrations need to be tested. Therefore, this HGurson model calibration procedure is cost efficient for engineering purpose.

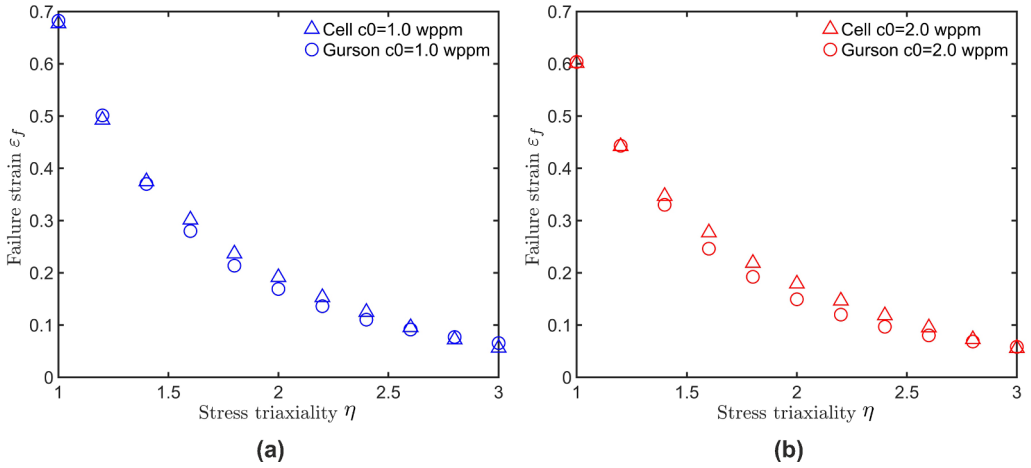

Fig. 7. Single element HGurson model prediction of hydrogen failure loci for (a) $c_0 = 1.0$ wppm and (b) $c_0 = 2.0$ wppm.

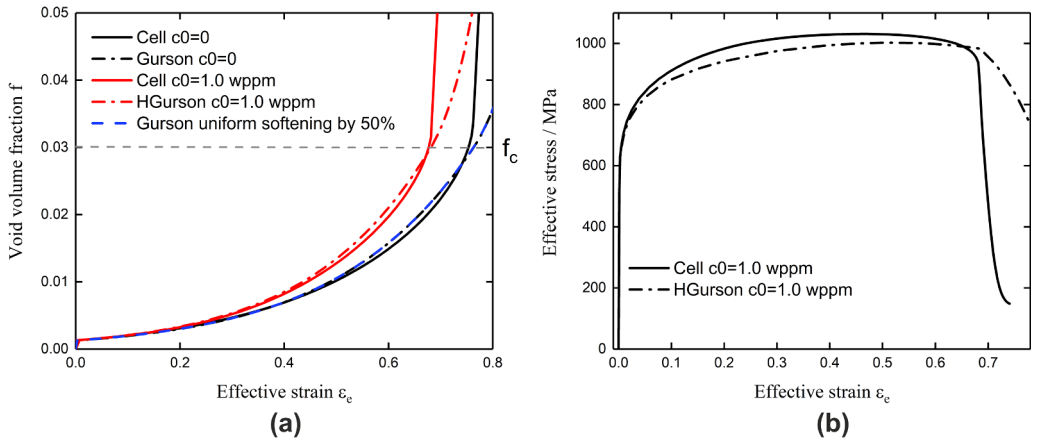

Fig. 8. The HGurson model prediction of (a) void growth curve and (b) effective stress-strain relation for the case with $\eta = 1.0$ and $c_0 = 1.0$ wppm. The void growth curves without hydrogen and a (artificial) void growth curve obtained by softening the original Gurson model uniformly are also included in (a).

4. Summary

A hydrogen informed Gurson model for hydrogen enhanced internal necking failure in high stress triaxiality regime was established in this work, as the first step towards a practical hydrogen embrittlement simulation tool based on the HELP mechanism.

Using hydrogen diffusion coupled unit cell analyses as "virtual experiments", hydrogen enhanced internal necking failure loci were constructed at various concentrations and an important conclusion in hydrogen-microvoid interactions, i.e. the decoupling principle, was drawn. The hydrogen failure strain was shown to be a decreasing function of stress triaxiality and hydrogen concentration, and more importantly, the effects of these two factors were found to be decoupled. Further investigation demonstrated that hydrogen caused non-uniform softening of the unit cell matrix is the dominant factor in hydrogen enhanced internal necking failure. These conclusions hold for a wide range of hydrogen trapping strength, as far as internal necking failure is concerned.

The HGurson model was proposed based these findings. Inspired by the decoupling concept, this model uses the Gurson model which accurately captures the hydrogen free microvoid process as the basis and introduces only one hydrogen related term to accelerate damage accumulation. Due to the clean formulation and the easy calibration of the hydrogen related term, the proposed model is user friendly and cost efficient for engineering practice. Good agreement between the HGurson model predictions and the "virtual experimental" results were achieved.

The HGurson model derivation was demonstrated using a strong hydrogen trapping case, since it gives pronounced hydrogen degradation in failure strain. In fact, we also studied the case with no hydrogen trapping and found that the model possesses the same form and follows the same derivation procedure. Therefore, this HGurson model is expected to apply to various hydrogen trapping strengths as far as internal necking failure mode is concerned.

This work concerns only hydrogen enhanced internal necking failure and is just the first step towards a HELP mechanism based hydrogen embrittlement simulation tool. To deliver a complete model applicable to the entire range of stress triaxiality, hydrogen induced internal shearing should also be addressed, which will be our next step.

Acknowledgements

The financial support from Aker Solutions and NTNU via the "Integrity of Ni-Alloys for Subsea Applications (INASA)" project is greatly acknowledged. We also want to thank the Research Council of Norway for funding through the "Hydrogen-induced degradation of offshore steels in ageing infrastructure – models for prevention and prediction (HIPP)". Contract No. 234130/E30.

Appendix A. Failure loci under milder hydrogen softening

In order to give a sense of how the magnitude of the effect of hydrogen depends on the softening parameters, we present the failure loci obtained using $\xi = 0.95$, $c_L^0 = 1.0$ wppm and $\xi = 0.99$, $c_L^0 = 1.0$ wppm (Eq. (2)). With milder hydrogen softening, the decrease in failure strain due to hydrogen becomes smaller. However, the shape of failure loci are the same as that in Fig. 1; it has been verified that the decoupling principle, e.g. Fig. 4 and Eq. (9) still holds. Therefore, the HGurson model formulation also applies in these cases with milder hydrogen softening (see Fig. A.9).

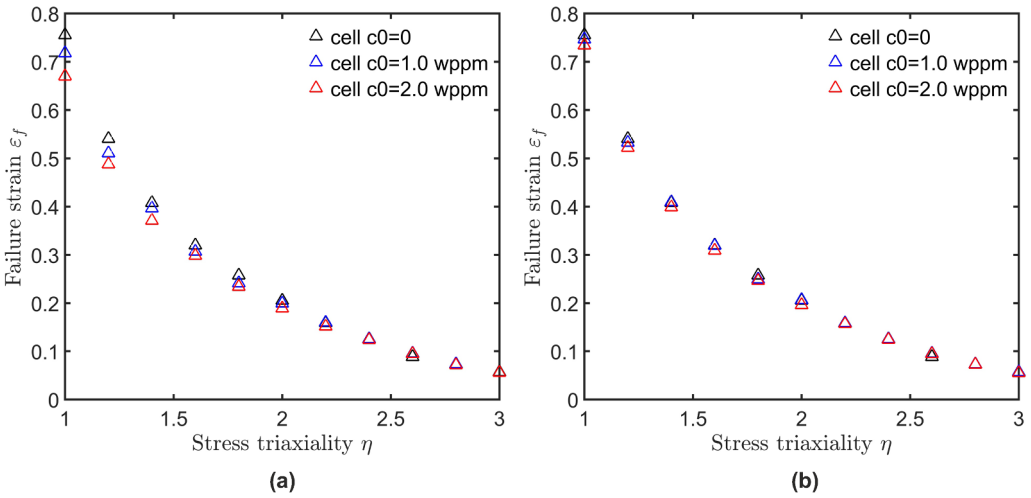

Fig. A.9. Failure loci obtained using unit cell analyses with milder hydrogen softening: (a) $\xi = 0.95$, $c_L^0 = 1.0$ wppm and (b) $\xi = 0.99$, $c_L^0 = 1.0$ wppm.

References

[1] Oriani RA. A mechanistic theory of hydrogen embrittlement of steels. Berich Bunsen Gesell Phys Chem 1972;76:848–57.
[2] Birnbaum HK, Sofronis P. Hydrogen-enhanced localized plasticity—a mechanism for hydrogen-related fracture. Mater Sci Eng A 1994;176:191–202.
[3] Yu H. Modelling and assessment of hydrogen embrittlement in steels and nickel alloys [PhD Diss]. Norwegian University of Science and Technology; 2003.
[4] Khoramishad H, Akbardoost J, Ayatollahi M. Size effects on parameters of cohesive zone model in mode i fracture of limestone. Int J Damage Mech 2014;23:588–605.
[5] Jiang DE, Carter EA. First principles assessment of ideal fracture energies of materials with mobile impurities: implications for hydrogen embrittlement of metals. Corros Rev 2004;52:4801–7.
[6] Serebrinsky S, Carter EA, Ortiz M. A quantum-mechanically informed continuum model of hydrogen embrittlement. J Mech Phys Solids 2004;52:2403–30.
[7] Olden V, Thaulow C, Johnsen R, Østby E, Berstad T. Application of hydrogen influenced cohesive laws in the prediction of hydrogen induced stress cracking in 25%Cr duplex stainless steel. Eng Fract Mech 2008;75:2333–51.
[8] Yu H, Olsen JS, Alvaro A, Olden V, He J, Zhang Z. A uniform hydrogen degradation law for high strength steels. Eng Fract Mech 2016;157:56–71.
[9] Alvaro A, Olden V, Akselsen OM. 3d cohesive modelling of hydrogen embrittlement in the heat affected zone of an x70 pipeline steel. Int J Hydrogen Energy 2013;38:7539–49.
[10] Pallaspuro S, Yu H, Kisko A, Porter D, Zhang Z. Fracture toughness of hydrogen charged as-quenched ultra-high-strength steels at low temperatures. Mater Sci Eng A 2017;688:190–201.
[11] Martínez-Pañeda E, Golahmar A, Niordson CF. A phase field formulation for hydrogen assisted cracking. Comput Methods Appl Mech Eng 2018;342:742–61.
[12] Ahn DC, Sofronis P, Dodds Jr RH. On hydrogen-induced plastic flow localization during void growth and coalescence. Int J Hydrogen Energy 2007;32:3734–42.
[13] Yu H, Olsen JS, He J, Zhang Z. Hydrogen-microvoid interactions at continuum scale. Int J Hydrogen Energy 2018.
[14] Yu H, Cocks ACF, Tarleton E. Discrete dislocation plasticity helps understand hydrogen effects in bcc materials. J Mech Phys Solids 2018.
[15] Gu Y, El-Awady JA. Quantifying the effect of hydrogen on dislocation dynamics: a three-dimensional discrete dislocation dynamics framework. J Mech Phys Solids 2018.
[16] Katzarov IH, Pashov DL, Paxton AT. Hydrogen embrittlement I. Analysis of hydrogen-enhanced localized plasticity: effect of hydrogen on the velocity of screw dislocations in α-Fe. Phys Rev Mater 2017;1:033602. PRMATERIALS.
[17] Sofronis P, Liang Y, Aravas N. Hydrogen induced shear localization of the plastic flow in metals and alloys. Eur J Mech A Solids 2001;20:857–72.
[18] Liang Y, Ahn DC, Sofronis P, Dodds Jr RH, Bammann D. Effect of hydrogen trapping on void growth and coalescence in metals and alloys. Mech Mater 2008;40:115–32.
[19] Koplik J, Needleman A. Void growth and coalescence in porous plastic solids. Int J Solids Struct 1988;24:835–53.
[20] Huang C, Gao X, Luo T, Graham SM. Modeling the effect of hydrogen on ductile fracture. Mater Perform Characteriz 2018;7.
[21] Gurson AL. Continuum theory of ductile rupture by void nucleation and growth: Part i—yield criteria and flow rules for porous ductile media. J Eng Mater Technol 1977;99:2–15. https://doi.org/10.1115/1.3443401.
[22] Tvergaard V, Needleman A. Analysis of the cup-cone fracture in a round tensile bar. Acta Metall 1984;32:157–69.
[23] Zhang ZL, Thaulow C, Ødegård J. A complete Gurson model approach for ductile fracture. Eng Fract Mech 2000;67:155–68.
[24] Zhang ZL, Niemi E. A new failure criterion for the Gurson-Tvergaard dilational constitutive model. Int J Fract 1994;70:321–34.
[25] Pardoen T, Hutchinson JW. An extended model for void growth and coalescence. J Mech Phys Solids 2000;48:2467–512.
[26] Nahshon K, Hutchinson JW. Modification of the Gurson model for shear failure. Eur J Mech A Solids 2008;27:1–17.
[27] Bao Y, Wierzbicki T. On fracture locus in the equivalent strain and stress triaxiality space. Int J Mech Sci 2004;46:81–98.
[28] Barsoum I, Faleskog J. Rupture mechanisms in combined tension and shear—micromechanics. Int J Solids Struct 2007;44:5481–98.
[29] Tvergaard V. Shear deformation of voids with contact modelled by internal pressure. Int J Mech Sci 2008;50:1459–65.
[30] Dunand M, Mohr D. On the predictive capabilities of the shear modified Gurson and the modified Mohr–Coulomb fracture models over a wide range of stress triaxialities and lode angles. J Mech Phys Solids 2011;59:1374–94.
[31] Xue L. Constitutive modeling of void shearing effect in ductile fracture of porous materials. Eng Fract Mech 2008;75:3343–66.
[32] Dæhli LE, Morin D, Børvik T, Hopperstad OS. A lode-dependent Gurson model motivated by unit cell analyses. Eng Fract Mech 2018;190:299–318.
[33] Manual AU. Version 6.13-2. Rhode Island, USA: Dassault Systémes Simulia Corp., Providence; 2013.
[34] Oriani RA. The diffusion and trapping of hydrogen in steel. Acta Metall 1970;18:147–57.
[35] Yu H, Olsen JS, He J, Zhang Z. Effects of loading path on the fracture loci in a 3D space. Eng Fract Mech 2016;151:22–36.
[36] Gurson A. Plastic flow and fracture behavior of ductile materials incorporating void nucleation, growth and coalescence [PhD Diss]. Brown University; 1975.

[37] Jiang W, Li Y, Su J. Modified GTN model for a broad range of stress states and application to ductile fracture. Eur J Mech A Solids 2016;57:132–48.
[38] Zhang ZL. Explicit consistent tangent moduli with a return mapping algorithm for pressure-dependent elastoplasticity models. Comput Methods Appl Mech Eng 1995;121:29–44.
[39] Zhang ZL. On the accuracies of numerical integration algorithms for Gurson-based pressure-dependent elastoplastic constitutive models. Comput Methods Appl Mech Eng 1995;121:15–28.
[40] Zhang ZL, Niemi E. A class of generalized mid-point algorithms for the Gurson–Tvergaard material model. Int J Numer Meth Eng 1995;38:2033–53.
[41] Kiran R, Khandelwal K. Gurson model parameters for ductile fracture simulation in ASTM A992 steels. Fatigue Fract Eng Mater Struct 2014;37:171–83.